Validation of Computational Models of Auxiliary Ventilation Systems with Experimental Data

K.W. Moloney,[1] D.M. Hargreaves,[1] I.S. Lowndes[1] and W. Pearce[2]
[1]School of Chemical Environmental and Mining Engineering (SChEME), University of Nottingham, England;
[2]Department of Aerospace Engineering, University of Bristol, Bristol

ABSTRACT

This paper reports the interim findings of a research program whose objective is to determine whether Computational Fluid Dynamic (CFD) models can be employed to accurately predict the airflow patterns within rapid development headings. In particular, the project aims to investigate the optimum set back distances for the ducts in order to adequately ventilate the face of the drivage. To validate the accuracy of the CFD model simulations measurements were obtained from a series of experiments performed on both scale models and within a full-scale surface gallery. The experimental scale-modeling program included making a series of pressure measurements across the face of the model for equivalent forcing duct setback distances of 5, 10 and 15 m (16, 33 and 50 ft). This pressure data was then plotted as contour plots and compared with the corresponding CFD predictions. A series of full-scale auxiliary ventilation trials were performed within a modified surface gallery. Three-dimensional velocity measurements were taken across a number of cross-sections using an ultrasonic anemometer. Velocity measurements were obtained for three forcing duct setback distances and for a typical force-exhaust overlap configuration.

KEYWORDS

Computational Fluid Dynamics (CFD), Scale Model, Pressure Measurements, and Auxiliary Ventilation.

INTRODUCTION

The provision of auxiliary ventilation to satisfactorily dilute and remove mine gases and dusts from dead-end headings is one of the more complex problems facing the mine ventilation engineer. The auxiliary ventilation system em-ployed should in no way affect the flow of air within the main ventilation system. The auxiliary ventilation system normally comprises of a combination of fan(s), ducting and/or brattice.

In the 1980s average drivage rates in single entry longwall development headings were 35m (115 ft) per week using steel arch sections. In the UK today, continuous miners can achieve typical advance rates of up to 100 m (328 ft) a week in rectangular section roof bolted roadways. Although the rates of advance have changed, ventilation practice has not. Current UK mining law requires that the primary ventilating air to the heading should be delivered to within 5 m (16 ft) of the face. This has led to the widespread adoption of auxiliary force-exhaust overlap ventilation systems, since a pure forcing system delivering the minimum of 4.5 m^3/s (9500 cfm) would lead to dust control problems at the head end.

An alternative solution to ventilate the heading would be to employ a forcing duct in conjunction with an exhaust scrubber fan mounted on the continuous miners. As the scrubber fan is not currently considered an effective primary ventilation system, the associated forcing duct has to be placed 5 m (16 ft) from the face. This arrangement does not produce a practical solution, as the force of the jet carries the dust past the scrubber inlets. This renders the exhaust scrubber system ineffective. Therefore, a conven-tional force/exhaust overlap ventilation system is normally employed within these headings (Yates, *et al.*, 1996). The ideal solution would be move the forcing duct back to an acceptable distance from the face such as to provide adequate methane control, whilst employing an on-board scrubber to provide dust control.

The principal objective of the current research programme was to determine whether CFD models could adequately predict the airflow patterns within an auxiliary ventilated heading. The results produced by the CFD models are to be assessed and validated against experimental data obtained from a series of scale model and full-scale surface gallery measurement programmes.

Previous research has demonstrated that the positioning of the outlet of a forcing duct at a distance of up to 15 m (50 ft) from the face of a coal drivage can augment effective methane control (Volkwein, *et al.*, 1985, Wesley, 1986).

INTRODUCTION TO CFD

Three fundamental physical principles govern the behaviour of any fluid flow: Newton's second law; the conservation of mass and the conservation of energy. These fundamental principles may be expressed in terms of a set of coupled partial differential equations known as the governing equations of fluid flow. Computational Fluid Dynamics (CFD) is a technique for determining a numerical solution for these equations. This is typically done by dividing the flow region into a large number of cells, which form a grid. In each of these cells, the governing equations are simplified and a solution process produces values of pressure, velocity and turbulence at the centres of these cells. It is thus possible to obtain a continuous solution throughout the domain by interpolating between these cell values.

The CFD models constructed and solved during the course of this study have employed two commercial solver packages, Fluent and CFX. Both packages have been shown to offer a similar range of modelling and processing facilities. Fluent was used during the scale model studies and CFX during the full-scale gallery studies. All numerical processing and validation studies were performed on a dedicated Sun Ultra 30 workstation.

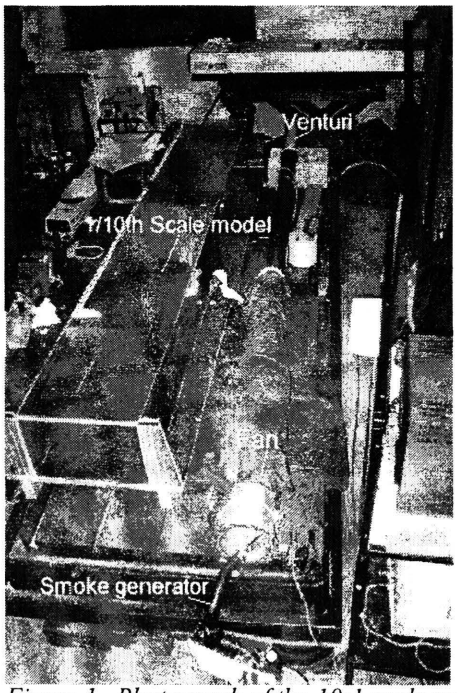

Figure 1. Photograph of the 10:1 scale model perspex model.

SCALE MODEL EXPERIMENTS

Scale Model

A 10:1 scale model of a typical UK longwall development heading was used to perform a series of pressure measurements across the face of the drivage (Figure 1). This model has been used for other work including Laser Doppler Anemometry (LDA) and Flow visualization studies and has been reported elsewhere (Moloney, *et al*,. 1998; Moloney, 1997).

Experimental Method

The face was drilled with 120 holes and tapped with hypodermic needles with an internal diameter of 2 mm (0.08 in). (Figure 2). The pressure measurements across the face of the model were taken using low range (+/- 10 mm (0.4 in) H_2O) differential pressure transducers. These transducers were calibrated using a Precision U-tube Manometer; graduated for readings down to 0.01mm (0.04 in) H_2O. These transducers had their positive side connected to pressure taps on the face of the gallery, whilst their negative side was connected a static pressure tapping on the forcing duct. Mean pressures were measured from time histories over a period of 60 seconds.

A pitot-static tube measured the velocity pressure within the delivery duct and was used as a reference to the

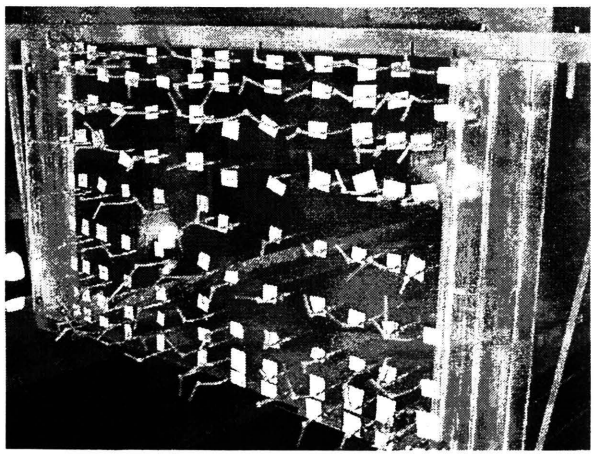

Figure 2. Picture illustrating the grid of pressure taps set across the face of the model.

determine the quantity of airflow entering the model. The pitot- static pressure was measured by a low-range differential pressure transducer with a range up to +/-20mm (0.78 in) H_2O. The measured face pressures were then divided by the reference pressure to normalise the data.
The experimental pressure data was represented by a series of contour plots, examples of which are illustrated below. (Figure 3).

The quantity entering the model through the duct was monitored by a BS venturi meter. The signals from the

measurement transducers were communicated to a PC computer via an A/D card. This data was electronically recorded and subsequently processed and analysed.

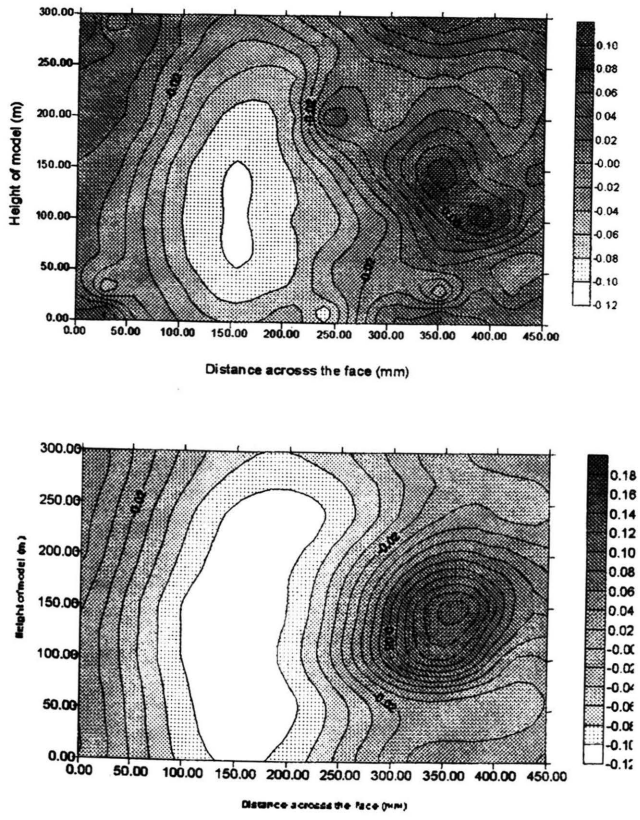

Figure 3. Comparison of CFD prediction (top) and experimental (bottom) for a pressure coefficient with the duct at 1 m (3.28) from the face.

Discussion

The high positive contour values observed to the right side of the two plots above represent the impingement of the forcing jet on the head-end. The negative contour values represent the movement of the ventilating airflow from the face of the model.

The experimental and predicted pressure contours illustrated above for the 10 m (33 ft) -configuration compare very favourably. The overall characteristics of high and low values are very similar and the envelope between the positive and negative pressure drops occurs in the same area. The actual pressure measurements compare quite well also albeit the CFD model produces slightly higher values within the jet region.

This experiment was repeated to simulate the outlet to the forcing duct being set at a distance of 5 m (16 ft) and 15m (50 ft) from the face. The data obtained from this series of tests resulted in a very similar series of flow characteristics between the measured and CFD predicted pressure regimes near the face.

FULL –SCALE EXPERIMENTS

Testing Facility

An existing surface training gallery was adapted in order to perform a series of full-scale auxiliary ventilation experiments. The original 65 m (213 ft) long arch section gallery is located at Welbeck Colliery in the village of Meden Vale, North Nottinghamshire. The gallery is constructed from a series of arched steel section supports, clad with galvanized steel sheeting and covered with grass seeded earth. The original gallery was extended at one end to form a 30m (98 ft) length of rectangular section roadway 4.75 m (15.5 ft) in width and 2.7 m (9 ft) high (Figure 4). A clean control room was constructed in the final three metres of the gallery behind the face.

Ventilation Studies

A series of experiments, employing three auxiliary ventilation configurations, were conducted within the surface gallery:

Force Ventilation System

The outlet to the eccentrically located duct was set at a distance of 5, 10 and 15 m (16, 33 and 50 ft) from the face of the gallery.

Force-Exhaust Overlap Ventilation. The force and exhaust duct outlets were set at distances of 15 m (50 ft) and 3 m (10 ft) from the face of the gallery respectively. The forcing quantity delivered was $6m^3/s$ (12,700 cfm) while the exhaust was $4m^3/s$ (8,400 cfm).

Controlled Re-Circulation System. The force and exhaust duct outlets were set at distances of 15 m (50 ft) and 3 m (10 ft) from the face of the gallery respectively. In this system, the forcing duct delivered 4 m^3/s (8,400 cfm) and the exhaust duct extracted 6 m^3/s (12,700 cfm).

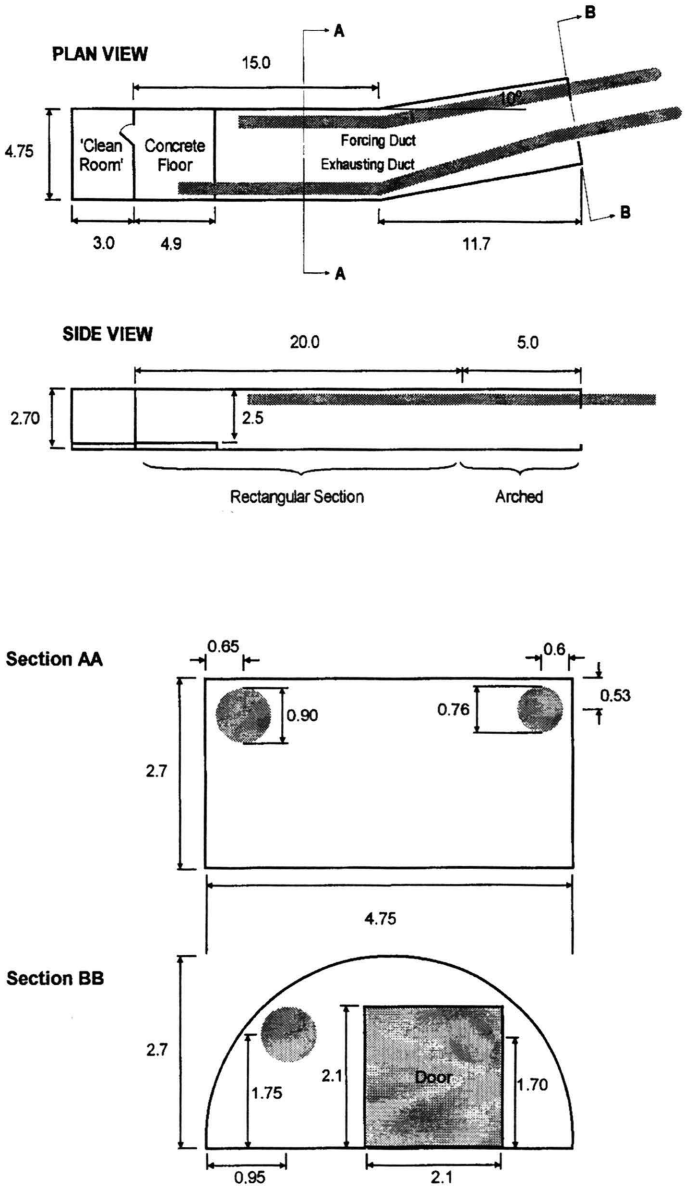

Figure 4. Sketch illustrating the full-scale test facility.

Ultrasonic Anemometer. A series of 3D velocity measurements were made within the gallery employing an ultrasonic anemometer. This anemometer comprises of a sensing head with six ultrasonic transducers arranged in pairs, surmounting a cylindrical electronic base housing (Figure 5). The velocity measurements were taken during a traverse of 25 grid points across a number of gallery cross-sections.

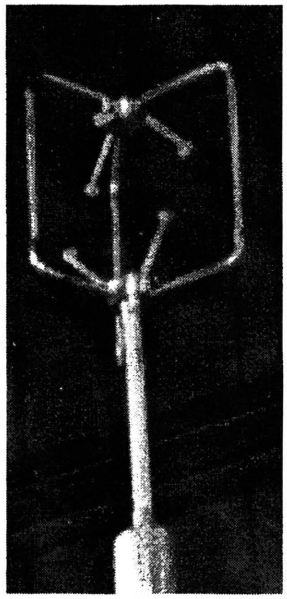

Figure 5. Picture illustrating the head of the Ultra-sonic anemometeter.

Processing. A sampling frequency of 20 hz was employed for the instrument, which resulted in 1048 samples over a period of 52.4 seconds for each of the u, v, and w components of velocity. A data logger recorded the measurements obtained from the ultrasonic anemometer in a compressed file format. These data files were imported into a spreadsheet to calculate the average and standard deviations of the three velocity components at each measurement point.

A flow visualisation package, AVS/Express, has been used to illustrate the results of the ultrasonic field measurements. The time-averaged mean values of the three measured velocity components (u, v and w) together with their standard deviations were calculated and specified at each measurement node of the grid.

Once the measured and computed data is imported into the AVS flow visualisation package. A series of different methods are available to the user with which to visualise the data. These include:

2D velocity contour plots taken across arbitrary planes defined through the 3D grid

3D iso-surface plots of the air speeds or turbulent intensities across the sampling grid

Vector plots (2 or 3D) of the flow velocities

Line plots of the velocity measurements taken along arbitrary traverses through the sampling grid

Figure 6 illustrates a typical graphical output that may be produced from the AVS/Express package. This plot illustrates a velocity vector plot with the forcing duct 10m (33 ft) from the face. A greyscale plot, although not as effective as colour, is still useful in the assessment of the general flow patterns within the heading. Also superimposed on the picture are manually created objects which represent the duct and the floor and walls of the gallery. The latter are given transparent shading to allow the vectors behind them to be seen more clearly.

The length of each vector is proportional to the time-averaged air speed measured at each point. The typical vortex and face scouring airflows can be seen clearly observed in Figure 6.

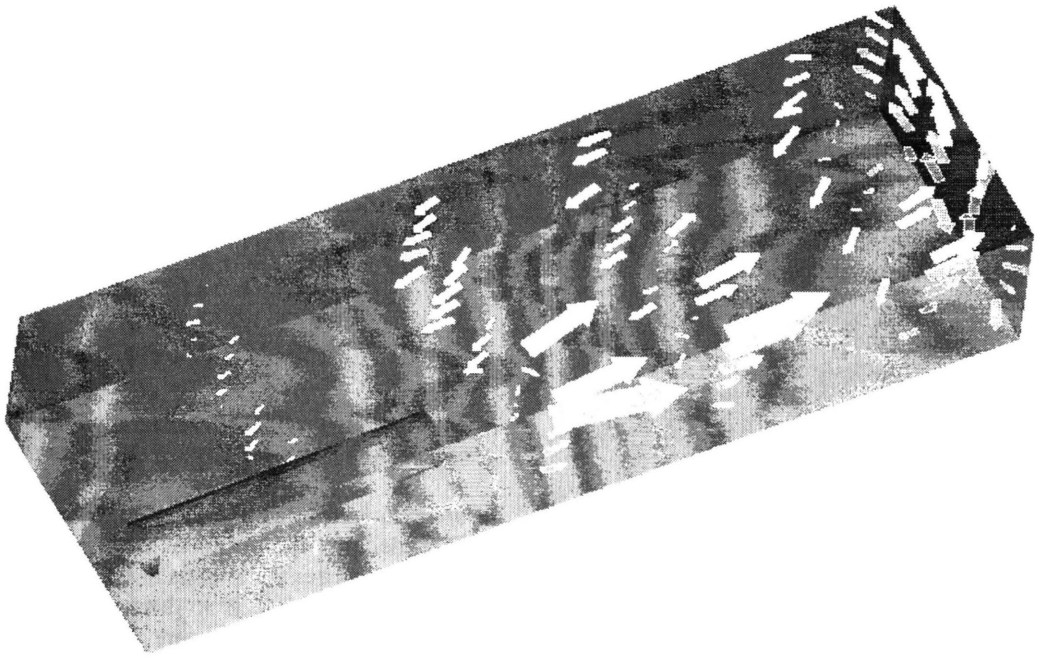

Figure 6. Example of velocity vector plot from Ultrasonic measurement program.

COMPARISON BETWEEN CFD AND FULL-SCALE

Before it is possible to use with confidence CFD to model such situations, there is a need to validate the CFD solutions with the data from a wide range of experimental studies. For each of the three auxiliary ventilation configurations employed at the Welbeck Gallery, a series of CFD models were constructed. Various features of the models were then altered in a systematic manner in order to obtain the best quantitative agreement between the experimental measurements and the solutions predicted by the model. The model design features that were varied included:

- wall roughness (duct, face, floor, roof and sides can be set independently),
- turbulence model (from a choice of k-ε, RNG k-ε, and differential Reynolds stress),
- grid refinement (in addition to a grid independence study).

Since the experimental anemometer measurements were restricted to the section of the gallery inbye of the bend, the CFD models of the forcing duct configurations were restricted to this region. However, to allow the flow to fully-develop within the forcing, the duct was modelled to extend a further 30 m out-bye. An average assumed duct wall roughness height of 0.01 m was found to produce best agreement with the experimental data. The rougher the wall

of the duct, the more concentrated is the predicted jet core which is emitted from the duct.

Figure 7 shows a predicted velocity vector plot for a modelled 10-m setback configuration for the forcing duct. This may be compared with Figure 6 that shows the measured anemometer data for the same situation.

Quantitative indications of the 'goodness of fit' are given in Figure 8, which show both experimental and CFD data across a typical traverse through the gallery, just in-bye of the duct exit. Only the *u*- and *w*-components of the flow are reproduced here in order to demonstrate the two extremes: very good agreement for the *u*-component; not so good for the *w*-component. Agreement also deteriorates close to the floor of the gallery – well out of the region affected by the jet.

It is also desirable to have a single measure of the difference between experimental data and each CFD job. An algorithm has been developed which quantifies the average difference between the two and produces a percentage error. This works by interpolating the CFD data to each of the measurement positions. It has proved to be a very effective aid to the CFD modellers.

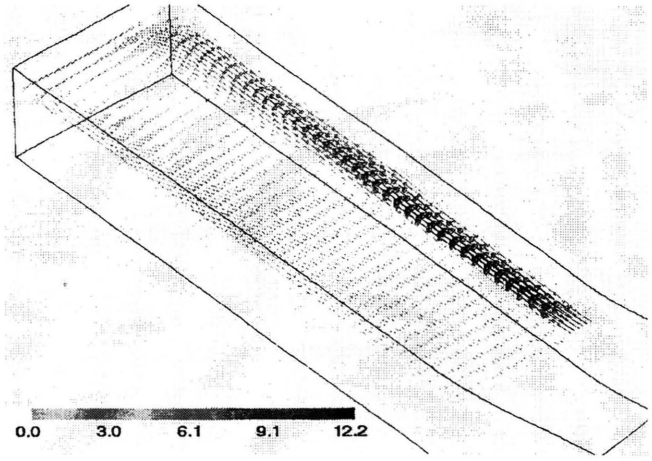

Figure 7. Velocity vectors from the CFD simulation of forcing duct at 10 m setback.

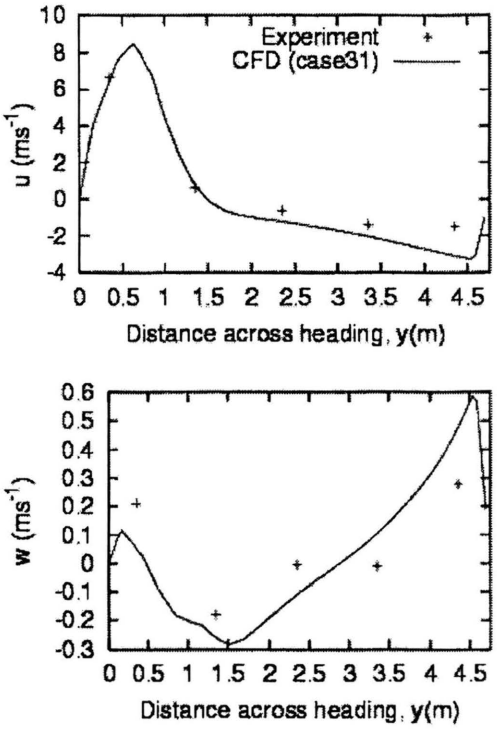

Figure 8. U- and w-components of flow for a traverse across the heading just in-bye of the duct inlet.

In order to justify the use of scale models (at least for the CFD modelling), the results of two simulations were compared. No changes were made to the geometry of either the scale or full-scale models so there was not exact geometric similarity. However, both were representations of the 15m setback forcing case. The major geometric difference was in the position of the duct relative to the walls. Modelling issues such as cell size and wall roughness were maintained at a ratio of 10:1 between full and scale.

The slight difference in duct position manifests itself in the results from the comparison. As in the case of Figure 8, these results (Figure 9) are from a traverse across the heading just in front of the duct outlet. The first plot is of the *u*-component (along heading) of the flow, normalised with the exit velocity at the centre of the duct. The across heading component of flow, *y*, is normalised by the width of the heading, *B*. The peak in the scale model results is displaced away from the wall at $y=0$, which would be expected as the duct was further away from the wall in relative terms. Otherwise, the two plots collapse well onto each other which goes some way to justifying the scale modelling. The second plot shows the pressure coefficient,

$$C_p = \frac{p}{\frac{1}{2}\rho u_0^2} \qquad (1)$$

where p is the total pressure and u_0 is the exit velocity. Here the agreement is not as good but this may be due to the slightly different positions of the duct more than any scaling issues. Critics of the k-ε turbulence model, which was used in this comparison, point to the fact that it can only model a single length scale of turbulence. This also may explain the differences. They are, however, not so great as to proscribe the use of scale models in investigations of the type described in this paper.

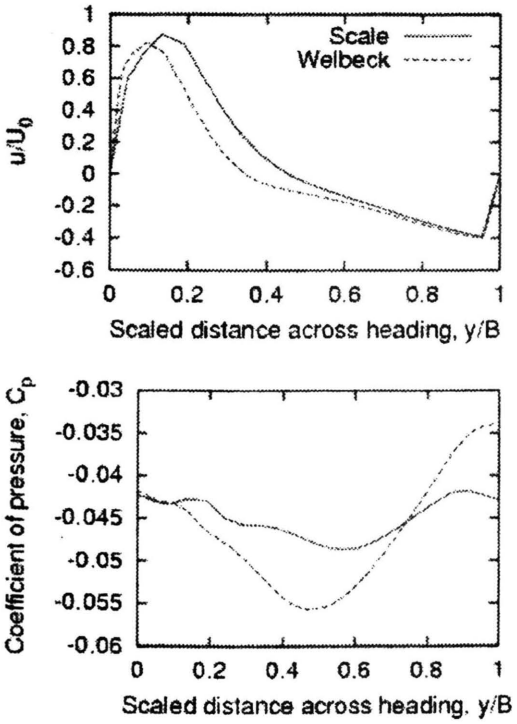

Figure 9. U-components of flow and coefficient of pressure for both scale and full-scale simulations along a transverse.

CONCLUSIONS

The CFD model predictions obtained from the model generally agree with the airflow patterns measured both within the scale model and within the full-scale gallery. It is clear that the CFD models produce superior predictions for flow regions exhibiting reasonable values of turbulence such as within the region of the forcing jet. However, the higher the turbulence intensity of and/or lower the air velocities the more inaccurate the CFD model predictions become.

REFERENCES

Moloney, K.W., (1997). "*An Analysis of Airflow Patterns in Auxiliary Ventilated Headings*," PhD Thesis, University of Nottingham.

Moloney, K.W., Lowndes, I.S. and Hargrave, G.K, "An Analysis of Airflow Patterns in Auxiliary Ventilated Headings," (accepted for publication, *Transactions of the Instn of Min Metall, Series A, Mining industry*).

Volkwein J.C., Thimons E.D. and Halfinger, G., (1985). "Extended Advance of Continuous Miner Successfully Ventilated With A Scrubber In A Blowing Section," *Proc 2nd US Mine Ventilation Symposium*, Mousset-Jones P. /ed./ 1 pp. 741-745.

Wesely, R., (1984), "Airflow at Heading Faces with Forcing Auxiliary Ventilation," *Proc. 3rd International Mine Vent Congress*, Harrogate, England, pp.73-81.

Yates, C., *et al.*, (1996), "Drivage Ventilation System at Welbeck Colliery," *Mining Technology*, December, Vol. 78, No. 904, pp. 319-324.